

## CHAPTER 3

### Experimental Procedures

This chapter presents the synthesis of films by using ultrasonic spray pyrolysis technique and the background of characterization technique for analysis the properties of films.

#### 3.1 Film preparation

##### 3.1.1 Substrate Cleaning

The substrate cleaning is the one important step before film coating. The powders, protein and fat were taken out form surface of substrates in this step. The substrates were cleaned using ultrasonic frequency with many chemical solutions in ultrasonic bath. There are 3 steps for cleaning. First, the substrates were immersed in 10% nitric acid solution for 30 min and washed with DI (Deionized) water. Then these substrates were washed again in ethanol solution and DI water. Finally these substrates were dried under a stream of air. The substrate cleaning process are shown in Figure 3.1

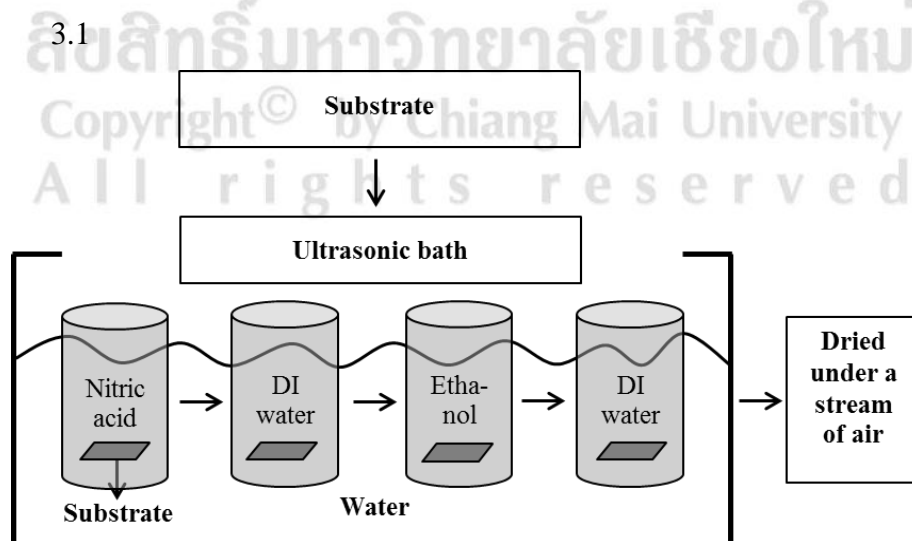


Figure 3.1 Schematic diagram of the substrate cleaning.

### 3.1.2 Film preparation

There are 2 steps of film preparation. First step was the starting solution preparation. The starting solutions were prepared from raw materials, which were dissolved in deionized water and ethanol. Moreover, hydrochloric (HCl) acid was added to increase the solubility of these solutions. Next step, the starting solutions sprayed on microscope glass substrates, which were heated at various temperatures in air. The distance between the ultrasonic nozzle and the substrate was 20 cm with nozzle frequency of 34 kHz and spray rate 2.5 ml/min. The schematic diagram of film coating is shown in Figure 3.2.

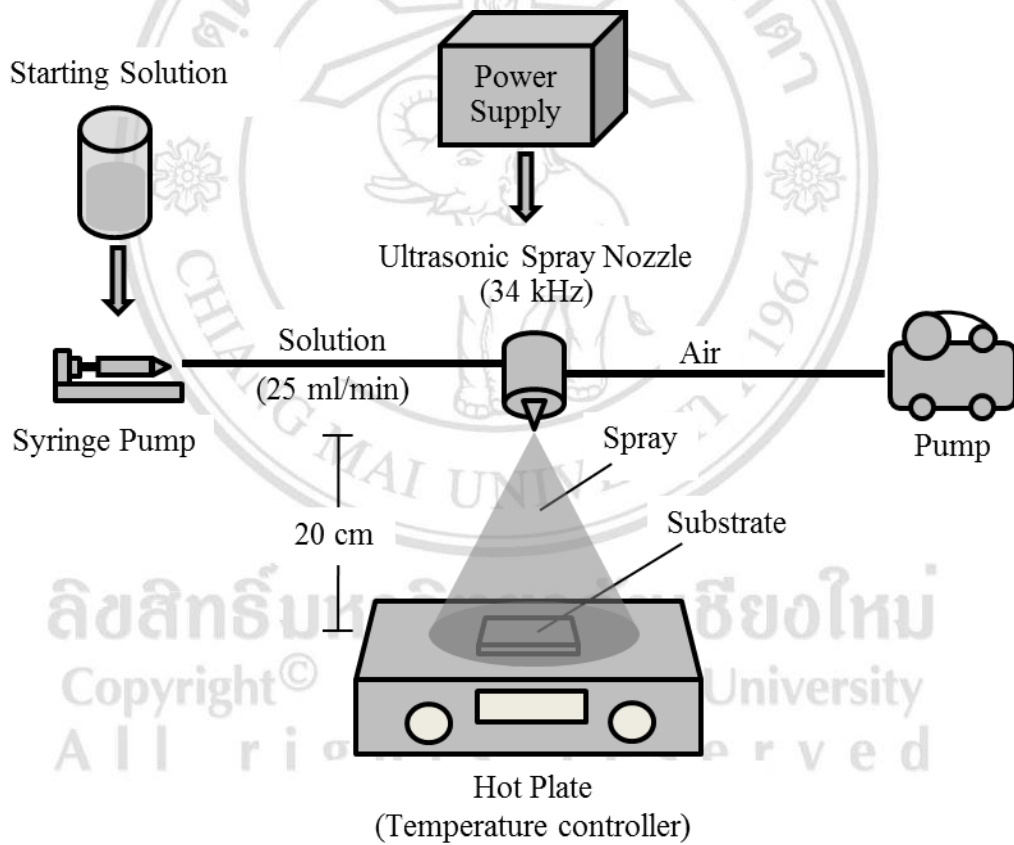


Figure 3.2 Schematic diagram of film coating.

### 3.2 Film Characterization

In this study, the properties of films such as crystalline phase, thickness, morphology, optical properties and electrical properties were characterized using X-ray diffractometer, scanning electron microscope, atomic force microscope, UV-Visible spectrometer and four point probe technique, respectively. The principle of these characterization techniques can be found in the following sections.

#### 3.2.1 X-ray diffraction (XRD) method [2,39,67-68]

XRD is a tool for identification of crystalline phase in materials (such as powder, film, polymer, glass and bulk materials). X-ray crystallography is a method of defining the arrangement of atoms within a crystal, the beam of X-ray attacks a crystal and scatters into many different direction. XRD is based on constructive interference of monochromatic X-rays and crystalline materials. The X-ray is generated by a cathode ray tube and filtered to monochromatic radiation. Then, this radiation is collimated to concentrate and directed toward the materials. The interaction of X-ray with materials indicate the crystalline phase of this material, according by Bragg's equation as follow

$$n\lambda = 2d_{hkl}\sin\theta_{hkl} \quad (3.1)$$

Where  $d_{hkl}$  is interplaner distance between (hkl) planes,  $\theta$  is angle of diffraction,  $\lambda$  is wavelength of incident X-ray and  $n$  is an integer. From diffraction geometry (Figure 3.3), the angle between the transmitted and diffracted beam will always be equal to  $2\theta$ . This angle can be obtained readily in experimental situations and results of X-ray diffraction are therefore given in terms of  $2\theta$ . Moreover, the angle is used in the Bragg's equation must correspond to the angle between the incident radiation and the diffracting plane.

The XRD pattern was recorded from X-ray diffractometer. The pattern is plot of scattering intensity versus the scattering angle ( $2\theta$ ), Example, the XRD pattern of ZnO powder is shown in Figure 3.4. The phases of materials are identified from the positions and intensities of peaks. Moreover, the

peak positions, intensities, widths and shapes of pattern explain the structure of materials. The XRD pattern data can be indicated the crystalline phase by compare with the Joint Committee on Powder Diffraction Standards (JCPDS).

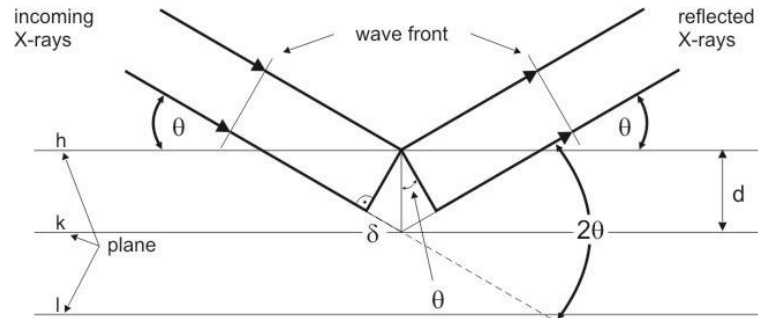


Figure 3.3 Scheme of the X-ray diffraction geometry [69].

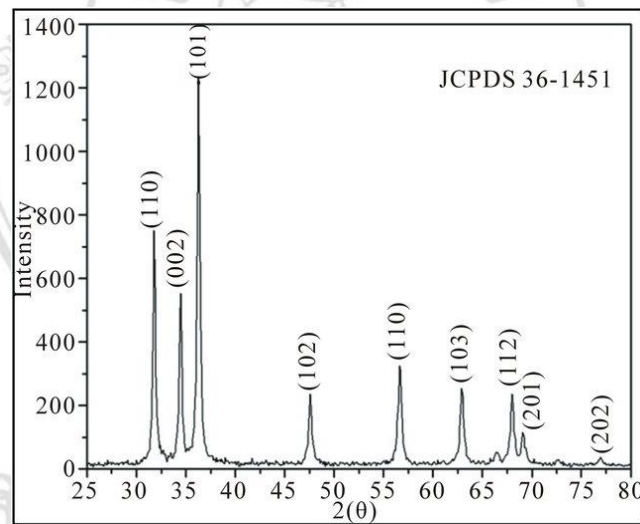


Figure 3.4 XRD pattern of ZnO powder [70]

Moreover, the full width at half maximum (FWHM) of preferentially oriented crystal plane can be indicated the crystalline size ( $G$ ) of materials, which is calculated using Scherrer's formular

$$G = 0.94\lambda/\beta\cos\theta \quad (3.2)$$

Where  $\lambda$  is the wavelength of X-ray,  $\beta$  = is the FWHM which has maximum intensity and  $\theta$  is the Bragg's diffraction angle

In this work, the X-ray diffraction diffractometer was investigated with the PANalytical, X' pert Pro MPD diffractometer (Figure 3.5). Monochromic  $\text{CuK}_\alpha$  radiation of wavelength  $1.54 \text{ \AA}$  was used to identify crystal phase of films and a scan step mode was used with a step size of  $0.001$  degree/second. Each sample was scanned from  $20$ - $80$  degree.

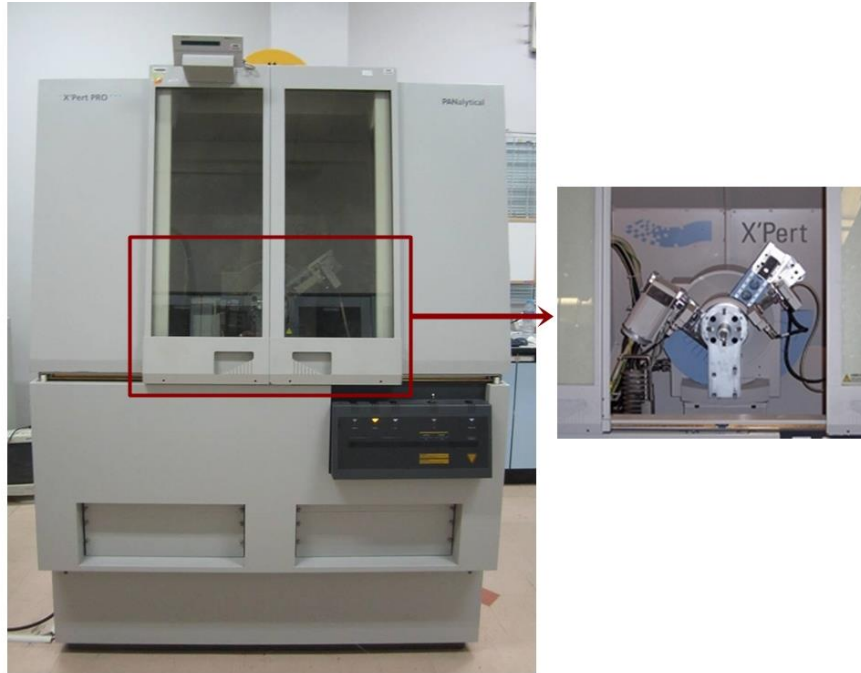


Figure 3.5 X-ray diffractometer (PANalytical, X' pert Pro MPD)

### 3.2.2 Scanning electron microscope (SEM) [2,39,68]

The SEM is a microscope that uses electrons to form an image. A beam of electrons (primary electron beam) is produced by an electron gun and focused by two condenser lenses into a beam with a very fine spot size. This beam then passes through the objective lens, where pairs of coils deflect the beam either linearly over a rectangular area of the sample surface. Schematic diagram of SEM is shown in Figure 3.6.

When the electron beam strikes the surface of the sample, this beam spreads effectively, fills a teardrop-shaped volume (interaction volume) which extends about  $1$ - $5 \text{ }\mu\text{m}$  into the surface (Figure 3.7). Secondary electrons are emitted from interaction in this region, which are then detected, converted to

voltage and amplified to produce an image. Moreover, the variety of other signals can be produced by SEM as Auger electrons, backscattered electron (BSEs), characteristic X-rays, continuum x-rays and fluorescence x-rays.

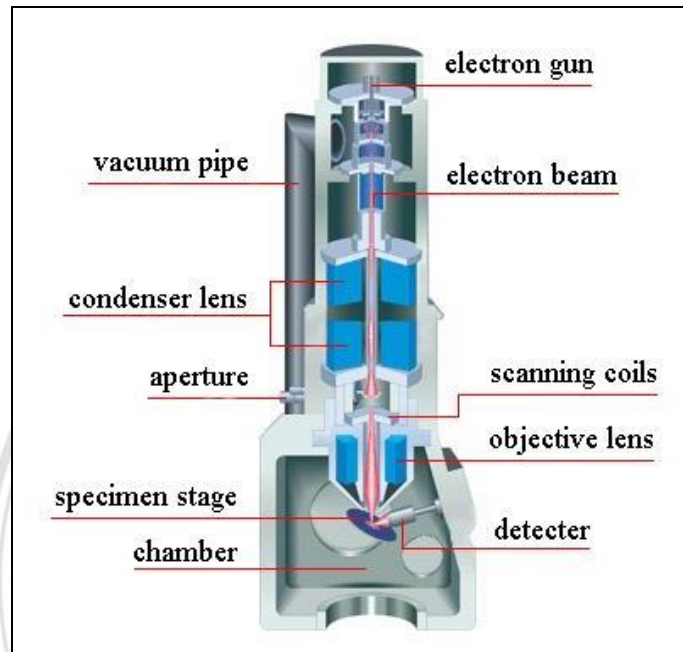


Figure 3.6 Schematic diagram of SEM [71].

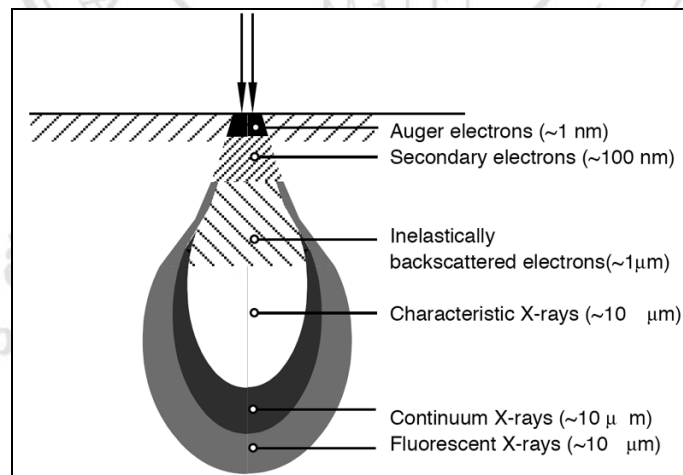


Figure 3.7 Electrons produced in SEM [72].

The samples are coated with a thin layer of conducting materials before analysis. This layer prevents charge build-up on insulating samples. Commonly materials are used as carbon coating that is most desirable if elemental analysis is priority, while metal coating (e.g. gold) is most

effective for high resolution electron imaging applications. Besides, the insulating sample can be examined without a conducting layer in an instrument capable of “low vacuum” operation.

Thickness of films was observed using scanning electron microscopy (SEM). A JEOL JSM-6335F field emission scanning electron microscope and a Quanta 200 3D Dual Beam Focused Ion Beam were used in this work and showed in Figure 3.8.



(a) JEOL JSM-6335F field emission scanning electron microscope



(b) Quanta 200 3D Dual Beam Focused Ion Beam

Figure 3.8 Scanning electron microscope.



### 3.2.3 Atomic force microscope (AFM) [39,68,73]

AFM is a one technique of scanning probe microscopes, which is used to images high-resolution surface structure on the range of nanoscale and to measure surface forces. The AFM contains a probe, laser and photodetector. The probe is a sharp tip, which is formed by silicon or silicon nitride with the curvature radius of  $\sim 10\text{-}50$  nm and attached to a cantilever spring. The Image of AFM tip is shown in Figure 3.9. When the tip is attracted on the surface, the forces between the tip and the sample lead to a deflection or vertical bending of the cantilever. This deflection is detected by a laser focused on the back of the cantilever and this laser is reflected onto a photodetector. The Principle of AFM showed in Figure 3.10. A plot of the laser deflection versus tip position on the sample surface gives the resolution of the hills and valleys that constitute the topography. This topography is also the description of shape and features of sample surface.

The most commonly used modes of operation of an AFM are contact, tapping and noncontact mode. Contact is static made, while tapping and noncontact is dynamic modes, as the cantilever is oscillated. This is mode done by adding a piezoelectric element that oscillates up and down at near the resonance frequency ( $\sim 300$  kHz) to the cantilever holder.

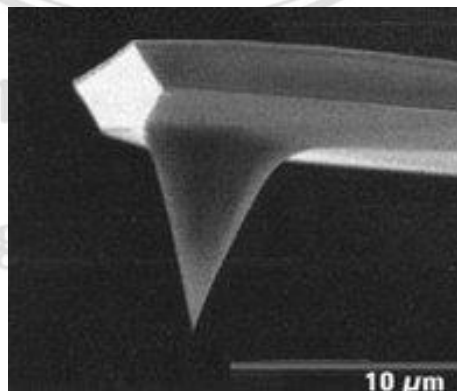


Figure 3.9 The Image of AFM probe [73].



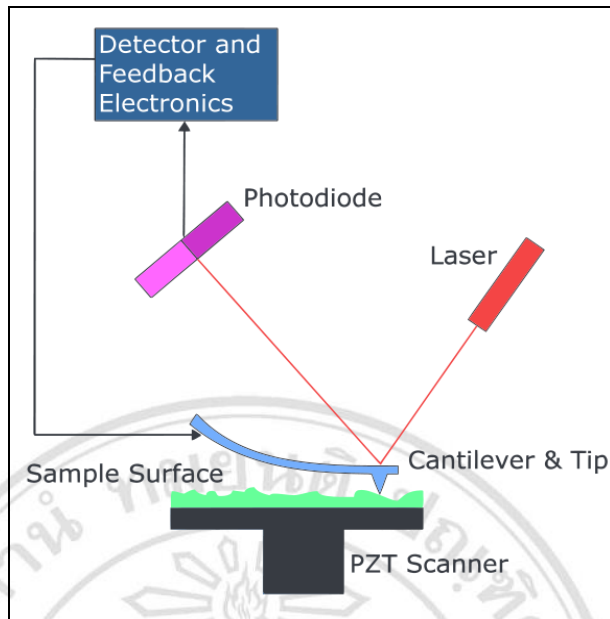


Figure 3.10 Principle of AFM [68].

Surface morphology, surface roughness and average grain size of films were analyzed by tapping mode AFM of a Nanoscope III Digital Instrument (Figure 3.11). The tapping mode AFM technique, the sample is scanned over by an extremely sharp tip at the end of a flexible cantilever. The attractive and repulsive force between the tip and surface can be detected. The microscopic image is obtained as a surface of sample, representing the locus of points of constant force between the tip and the sample.



Figure 3.11 Digital Instruments Nanoscope III Scanning Probe Microscope.

### 3.2.4 UV visible spectrophotometer [22,39,61,68]

Ultraviolet (UV) and visible (VIS) radiation are a small part of the electromagnetic spectrum (Figure 3.12). The energy ( $E$ ) associated with electromagnetic radiation is defined by equation:

$$E = h\nu \quad (3.3)$$

where  $h$  is plank's constant ( $6.62606957 \times 10^{-34}$  J.s or  $4.135667516 \times 10^{-15}$  eV.s) and  $\nu$  is photon frequency. Electromagnetic radiation moves through space with a wave motion because radiation acts as a wave, it can be classified in terms of wavelength ( $\lambda$ ) or frequency by equation:

$$\nu = c/\lambda \quad (3.4)$$

where  $c$  is the speed of light ( $3 \times 10^8$  m/s).

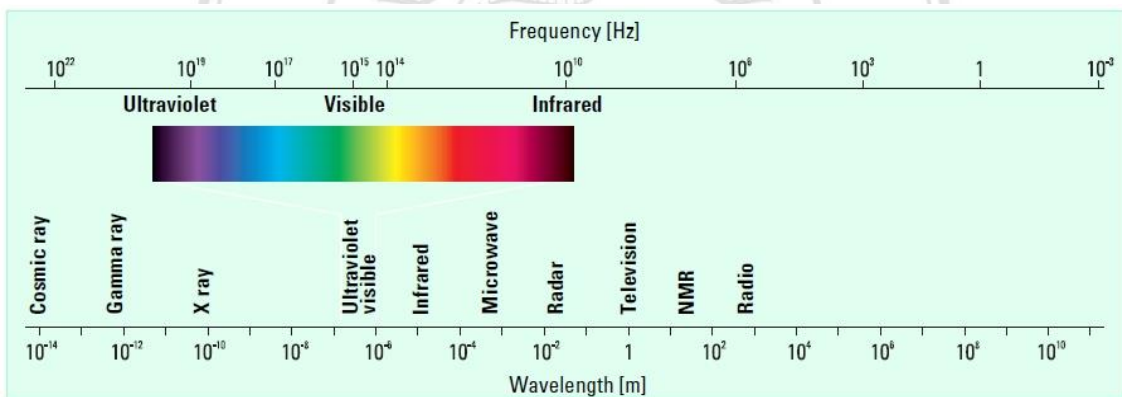


Figure 3.12 Electromagnetic spectrum [74].

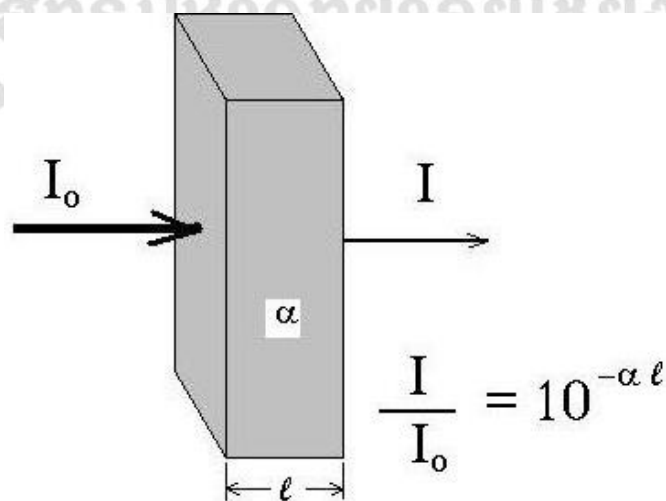


Figure 3.13 Schematic diagram of the absorption process [75].

When light passes through a sample, the difference between the incident radiation ( $I_0$ ) and the transmitted radiation ( $I$ ) is the amount of light absorbed (Figure 3.13), which is expressed as either transmittance ( $T$ ) or absorbance ( $A$ ). Transmittance usually is given in terms of a fraction of 1 or as a percentage. Transmittance defined as follows:

$$T = I/I_0 \quad (3.5)$$

or

$$\%T = (I/I_0) \times 100 \quad (3.6)$$

And absorbance defined as follows:

$$A = -\log T \quad (3.7)$$

The band gap ( $E_g$ ) was evaluated from the transmittance spectra using Tupaç's relationship [61]. This relationship was related between the absorption coefficient ( $\alpha$ ) and the photo energy ( $h\nu$ ). i.e.,

$$\alpha = B(h\nu - E_g)^n/h\nu \quad (3.8)$$

where  $B$  is a constant and  $n$  is 1/2 for direct band gap, semiconductor material is a direct band gap [61]. The absorption coefficient is obtained from the transmittance and thickness ( $t$ ) by using Beer's law [22]. The relationship defined as:

$$\alpha = -(1/t)\ln T \quad (3.9)$$

Thus, the absorption coefficient as a function of the photon energy was calculated. The intercept of  $(\alpha h\nu)^2$  on the  $x$ -axis gave the value of the direct band gap.

In this work, the films were used UV visible spectrophotometer with an integrating sphere of PerkinElmer Lambda 35 UV/VIS Spectrophotometer (Figure 3.14) in wavelength of 300-1000 nm.



Figure 3.14 PerkinElmer Lambda 35 UV/VIS Spectrophotometer.

### 3.2.5 Four point probe technique [2]

A four point probe technique is a sample way to analysis the electrical properties of thin films by determining the sheet resistance ( $R_s$ ). This technique consists of four probes with equal spacing  $\sim 1$  mm (Fig 3.15). By applying the current through the outer terminal and measuring the voltage across inner terminal, the sheet resistance will be determined. Knowing the films thickness ( $t$ ), then the resistivity ( $\rho$ ) can be calculated following the equation 3.10

$$R_s = \rho/t \quad (3.10)$$

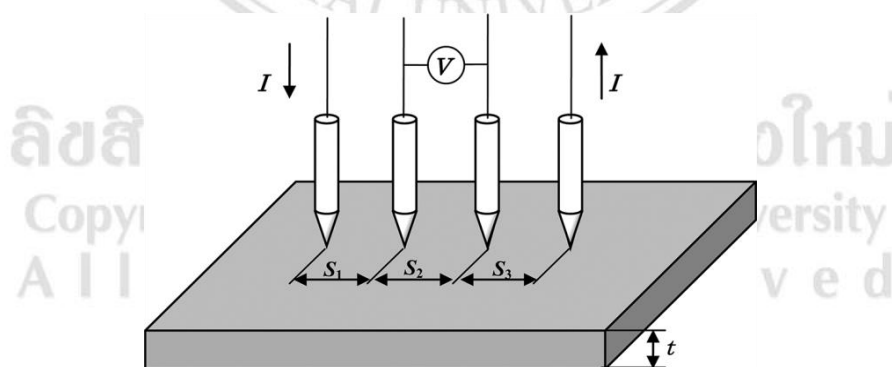
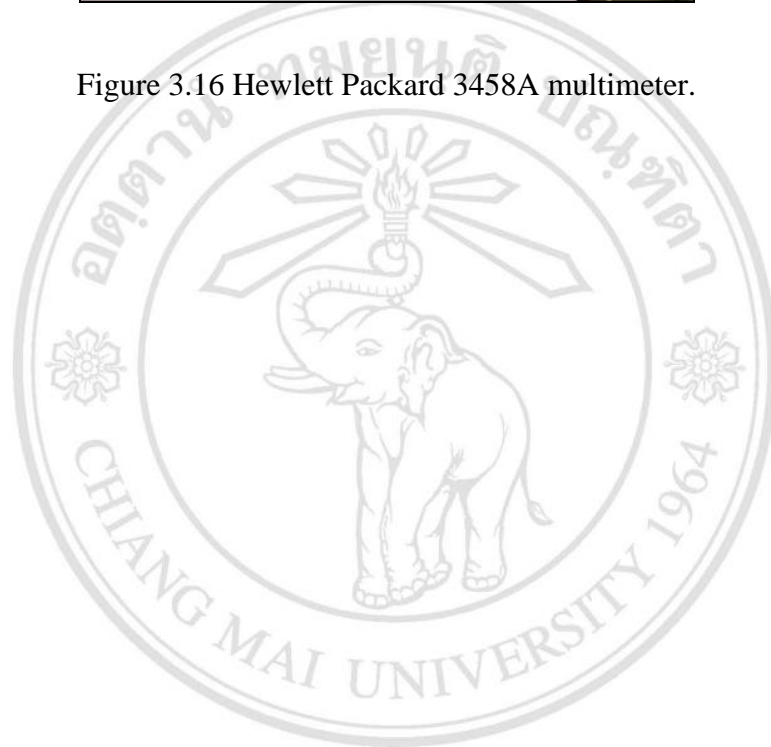


Figure 3.15 Four point probe technique [76].

In this work, the sheet resistance of films was measured by digital multimeter (Hewlett Packard 3458A multimeter) with four point probe. The digital multimeter showed as Figure 3.16.



Figure 3.16 Hewlett Packard 3458A multimeter.



ลิขสิทธิ์มหาวิทยาลัยเชียงใหม่  
Copyright© by Chiang Mai University  
All rights reserved